Study of Antifungal Activity Using Three Chinese Medicine Herbs

Anming Zhu Shiming Ren Xueqi Li Xiaoqi Zhao
Lei Wang Minzhen Bao Yamei Wang

Abstract

Chinese medicine herbal extracts are ideal candidates to replace toxic industrial wood preservatives thanks to their antifungal and nontoxic properties. To investigate the antifungal activity of Chinese herbal medicines, in this study, *Trametes versicolor* fungi were selected as test strains to evaluate the antifungal properties of Fructus Cnidii, Fructus Forsythiae, and Radix Stemonae. The results show that Fructus Cnidii has a strong inhibitory effect against *T. versicolor*, whereas Fructus Forsythiae and Radix Stemonae have a weak inhibitory effect. The hyphae growth cycle shows that the three studied Chinese herbs disrupt the growth of *T. versicolor*. Moreover, instead of direct killing, the Chinese herbal medicine demonstrated inhibition ability. Furthermore, the morphological and toxicological evidence shows that Fructus Cnidii affected the expression of proteins or enzymes to achieve the inhibition goal. In sum, this study could provide both primary data and a theoretical foundation for further developing and applying for traditional Chinese medicine as a green type of wood preservative.

As an environmentally friendly material, wood is indispensable in human life and industrial production and is widely used in the building material and furniture industries (Shen et al. 2018, Teng et al. 2018). The efficient and cost-effective use of wood is linked to the long-term development of the global economy and society. In this context, anti–wood decay (wood preservation) is one of the most effective methods for efficiently using forest resources (Macchioni et al. 2016, Broda 2020, Penttilä et al. 2020).

Traditionally, the toxicity of heavy metals such as Hg, Cu, and Ni (Baldrian 2003) has been applied to produce antifungal wood preservatives because heavy metals can regulate ligninolytic and cellulolytic transcription levels. However, the overuse of heavy metals can cause health risks for humans and animals because of its nondegradable and cumulative behaviors. On the other hand, chemicals such as cinnamaldehyde and eugenol also have been used to explore the antifungal ability with white and brown rot. Nevertheless, currently, the cost of these chemicals is not suitable for industry utilization. As more attention is paid to the ecological environment around the world, the development of nonpolluting wood preservatives with low toxicity, low cost, and good environmental compatibility with organisms is a growing research topic (Khan et al. 2001a, 2001b; Sinha et al. 2001).

Previous research has demonstrated that Chinese herbal medicines have a high development value as an antifungal material due to their naturalness and lack of toxic heavy metals (e.g., chromated copper arsenate) (Khan et al. 2002, Green and Clausen 2003). China is blessed with a large and diverse range of herbal medicine resources that have been utilized in food preservation and livestock feed additives, resulting from years of research and application (Ekor 2014). Therefore, developing a new type of wood preservative based on green and pollution-free Chinese herbals has a high likelihood and far-reaching implications in wood preservation.

Fungi-caused wood decay is the most common type of wood decay and comes in three varieties: white, brown, and soft (Goodell et al. 2008). According to previous studies, various Chinese herbal medicines, such as *Coptis chinensis*, Sichuan pepper, and saponin, have been screened out with good antifungal effects on wood decay fungi (Jiang et al. 2014). Moreover, *Gleditsia sinensis* and Sichuan pepper

The authors are, respectively, Graduate Student, Graduate Student, Graduate Student, Graduate Student, and Graduate Student, College of Materials Sci. and Art Design, Inner Mongolia Key Lab. of Sandy Shrubs Fibrosis and Energy Development and Utilization, Inner Mongolia Agric. Univ., Hohhot, China (844239445@qq.com, 1305625858@qq.com, 3448220368@qq.com, zxiaoqi219@163.com, wanglei792@163.com); Assistant Professor, China National Bamboo Research Center, Hangzhou, China (baominzhen@caf.ac.cn); and Professor, College of Materials Sci. and Art Design, Inner Mongolia Key Lab. of Sandy Shrubs Fibrosis and Energy Development and Utilization, Inner Mongolia Agric. Univ., Hohhot, China (Wangym80@126.com [corresponding author]). This paper was received for publication in April 2021. Article no. 21-00027.

Forest Prod. J. 71(4):322–329.
doi:10.13073/FPJ-D-21-00027

were found to be the most effective Chinese herbal medicines against *Coriolus versicolor* (white rot), while *G. sinensis* was the most effective against *Monilinia fructicola* (brown rot) (Goodell 2003). *C. chinensis* was the most effective Chinese herbal medicine with a more substantial antimicrobial effect than *G. sinensis* and Sichuan pepper (Jiang et al. 2014). Although many Chinese herbal medicines with good antifungal effects on wood-rot fungi have been discovered, such as coptis root, pericarpium zanthoxyli, and Chinese honeylocust fruit, among others (Jiang et al. 2014), there have been few in-depth studies on the underlying mechanisms. In general, by affecting the fungi's metabolism and physiological activities, drug inhibition often has a devastating effect on the fungi's structure or physiology. The sequence of destruction of the fungi structure could be classified as action on cell walls, causing structural damage to cell walls and the leaking of contents (Khan et al. 2001b, 2002). In addition, the effects on metabolism and physiological activities can be classified as effects on the enzyme system, respiratory inhibition, and mitosis. Antifungal agents on microorganisms do not have a single action; they can act on multiple aspects simultaneously, or they can act on only one side but produce a series of effects.

To the best of our knowledge, most of the previous literature has focused on brown-rot fungi (Green and Highley 1997, Jellison et al. 1997), and the lack of research on white-rot fungi has resulted in the obscurity of its rot mechanism. Typically, white rot is often associated with hardwood decay, which possesses both cellulolytic and ligninolytic, makes the wood express a bleached appearance, and has a spongy structure (Goodell et al. 2008), which is different from brown rot and soft rot. As a result, research into the growth law, morphology, and process mechanism of white-rot fungi is critical for developing a renewable, environmentally friendly, nontoxic, and biodegradable wood preservative.

In this study, the antifungal activity of three Chinese herbals was investigated. Isoelectric focusing electrophoresis, SDS-PAGE electrophoretic analysis and staining, and scanning electron microscopy, among other methods, were used. The objectives of this study were to (1) determine whether the selected Chinese herbal medicines have a good inhibitory effect on *Trametes versicolor*; (2) investigate whether the selected Chinese herbs affect the *T. versicolor* growth cycle and, if so, how; (3) examine the changes in mycelium morphology caused by herbal medicines; and (4) investigate whether herb action has affected mycelium's function in regulating the DNA synthesis of proteins or enzymes.

Materials and Methods

Strain and extraction

The white-rot fungus *T. versicolor* (L.) Lloyd (TV) was bought from the Chinese Academy of Forestry's Institute of Forest Ecological Environment and Protection and was cultured and activated in the laboratory using a PDA plate medium. Fructus Cnidii (FC), Fructus Forsythiae (FF), and Radix Stemonae (RS) were purchased from Guoda Pharmacy (Hohhot, Inner Mongolia). The three types of Chinese herbal medicines were crushed through 80 mesh, weighed, and soaked for at least 2 hours in distilled water. A hydrothermal decocting process was used to extract each sample, and the residue was filtered to obtain the water extract, which was concentrated to 1.0 $\pm$ 0.005 g/mL.

PDA medium

The peeled and washed potatoes (200 g) were cut into small pieces and boiled for 30 minutes in water before being filtered with gauze. Then the water, 18 g glucose, and 18 g agar were added to 1,000-mL solutions, boiled until the agar dissolved entirely, and plated. Next, the prepared culture medium was sterilized in a high-pressure steam sterilizer for 30 minutes under 0.1 MPa and 121°C and then placed on a vertical flow clean bench and irradiated with an ultraviolet lamp while cooling. Finally, the poisoned plate or liquid medium was prepared by adding the Chinese herb extract (5 mL) and cooling it to about 50°C in an aseptic environment.

Antifungal testing

A hole punch was used to take a 5-mm-diameter stalk from the 5-day cultured TV, and the stalk was inoculated onto the toxic plate medium and nontoxic control medium with fungus facedown. The plates were incubated for 7 days in a constant incubator at 27°C and 78% relative moisture. The microbiome diameter was measured with a Vernier caliper every day, and the growth (fungal circle) was recorded to calculate the growth rate. The inhibitory efficiency of three Chinese herbs on TV was calculated using the following formulas:

$$G_D = \frac{(C_D - C_{D-1})}{C_{D-1}} \times 100\% \quad (1)$$

Here, G_D is the growth rate of the fungal circle at day D, $1 < D \leq 7$, and C_D is the diameter of the fungal circle at day D:

$$I_D = \frac{(D_D - T_D)}{D_D} \times 100\% \quad (2)$$

Here, I_D is the inhibitory effect of herbs on TV at day D, $1 \leq D \leq 7$; D_D is the diameter of the fungal circle in blank control medium at day D; and T_D is the diameter of the fungal circle in the toxic medium at day D.

The data were repeated three times in each group, and their arithmetic averages (differences less than 10%) were used.

Determination of growth period

The change in cell number can reflect the growth law of microorganisms. Within a specific range, microbial cell concentration is inversely proportional to transmittance and directly proportional to optical density (OD). As a result, the OD of fungus suspension can be determined using an ultraviolet spectrophotometer. To observe the change in microbial cell number, continuous measurements can be plotted against the corresponding culture time. Under aseptic conditions, the fungus block with a diameter of 5 mm was added to the toxic and nontoxic liquid media and cultured in an HZ100L Vertical Constant Temperature Shaker at 27°C for 5 days. The OD of each group was measured using a TU-1901 UV-Vis spectrophotometer, and the uninoculated liquid medium was used as the control sample to plot the growth curve.

Morphology observation

To avoid sample shrinkage caused by dehydration and drying, resulting in changes in mycelium surface morphology and even the destruction of mycelium structure, ethanol with low surface tension was used to replace water with high surface tension. Thus, the drying process had less impact on the sample surface. The samples were dried in the HCP-2 critical point drying instrument using the critical point drying method, eliminating the source of surface tension. Several pieces of fungi near the colony's fringes were chosen under aseptic conditions after TV was cultured on poisonous and nontoxic blank plate media for 5 days. After fixing, cleaning, dehydration, substitution, critical point drying, and gold plating (BAL-TEC SCD 005 low-temperature sputter coater), all the samples were examined under an XL30 ESEM-FEG environmental scanning electron microscope.

Protein sample preparation

The fungal block samples were cleaned with 1:1 ethanol/ether solution and centrifuged. First, 10× volume 10% TCA-acetone solution was used to dissolve the sediment and mixed with lysis solution (0.1 M PMSF, 0.2 M EDT A, 1 M DTT). Then ultrasonic treatment was conducted for 1 minute, 2 seconds/3 seconds, and cracking at −20°C for 2 hours and centrifugation at 4°C for 35 minutes. Next, the precipitate was suspended 10 times the acetone solution volume and again mixed with the lysis solution. Ultrasonic centrifugation of the preceding operation was repeated twice. Finally, all organic solvents were removed after vacuum drying the precipitate for 5 minutes.

According to the proportion of 200 μL of protein, leaching liquor of a 10-mg sample (8 M urea, 4% CHAPS, 0.5% to 2%, pH 3.5 to 9.5, amphoteric electrolyte, 40 mM Tris base pH 8.5) was mixed with lysis solution and ultrasonicated for 5 minutes, 2 seconds/3 seconds, then fully dissolved for 1 hour at 10°C and centrifuged at 3,000 × *g* for 25 minutes. The resulting supernatant was the protein solution, and its protein concentration was determined using the improved Bradford method.

Isoelectric focusing electrophoresis

In this study, an Amersham IPGphor apparatus was used. The sample volume was 100 μL, and the parameters were set as 50 V hydration for 12 hours (17°C), 250 V for 1 hour, 1,000 V for 1 hour, 10,000 V for 5 hours, and 500 V for 10 hours, respectively. After processing, the tapes were balanced, and two-dimensional SDS-PAGE electrophoresis was performed immediately. Then the tapes were placed in the sample hydration plate at −70°C.

SDS-PAGE electrophoretic analysis

An electrophoresis apparatus (Amersham Ettan II) was used in this study. Low-current (5 mA) electrophoresis was run on the sample initially, and when the sample was entirely out of the IPG strip and concentrated into a line, the current was increased to 20 to 30 mA. The electrophoresis is terminated when the bromophenol blue indicator reaches the bottom edge. The gel was then removed from the cast for silver staining.

Map scanning and analysis

After gel coloring, the two-dimensional electrophoresis images were scanned by an Amersham PowerLook 2100XL gel imager. ImageMaster 2D platinum 5.0 was used to analyze the protein differences of the two different conditions.

Results and Discussion

Growth of *T. versicolor*

In general, single-celled microorganisms growing in a specific environment follow a set of rules representing the entire process of growth and reproduction in a suitable environment. There are four stages—lag, logarithmic, stationary, and decline—in a standard growth curve (Zwietering et al. 1990, Wachenheim et al. 2003).

Figure 1 depicts the growth characteristics and inhibition efficiency of *T. versicolor* (TV) cultured in various media between days 3 and 7. With increased culture time, the diameter of TV increased for all media (Fig. 1a). In addition, based on the diameter of the TV circle, the antifungal activity showed RS = FC < FF < control (CO) on day 3 and FC < FF < RS < CO from day 4 to day 6 but FF < FC < RS = CO on day 7. These results indicated that the antifungal ability of FC was better than the other two media in the early stage. However, the antifungal ability may be decreased with prolonged culture time; for example, TV's diameter on day 7 in different media showed RS = CO and FC > FF.

Figures 1b and 1c provide the initial growth rate and inhibition rate of TV in different media. The growth rate of RS showed an exponential trend from day 3 to day 6, indicating that the fungi were rapidly developed. The water extract may explain this result because it provided nutrients to accelerate the TV growth in the subsequent growth process. Although the growth rate of FF gradually decreased, the initial growth rate was higher than that of RS and FC. As shown in Figure 1c, the inhibition efficiency of FF and FC increased first and then decreased, a normal phenomenon indicating the loss of drug efficiency due to the development of resistance. Moreover, the inhibitory effect of FC was significantly better than that of RS.

Figure 1d presents the OD of TV with different bases. The initial OD values of the four conditions are different, which is explained by the color difference of the Chinese herbal extract, and this would not affect the experimental results. When the TV grows on the blank culture medium, each phase can be observed clearly, and the decline phase was not significant because it cannot distinguish between dead and living fungi. However, the growth curve of TV growing in a poisonous medium changed due to the antifungal effect of FC, FF, and RS. In addition, there was no delay period for TV treated with FC, and it directly entered a short logarithmic phase, followed by a long period of stability and decay. On the other hand, the TV treated by FF crosses the logarithmic phase from the delay period to the stable phase and subsequently the decay period. After rapid growth in the logarithmic period, the white-rot fungus treated by RS enters the slow growth process, with no signs of decay, indicating that the growth inhibition of RS was weak. Figure 2 compares the growth status of TV in the blank culture medium and FC culture medium on day 6, showing an excellent antifungal ability with FC.

Scanning electron microscopic analysis

The mycelium of white-rot fungus in the blank control was slender, full, and uniform in thickness, with few

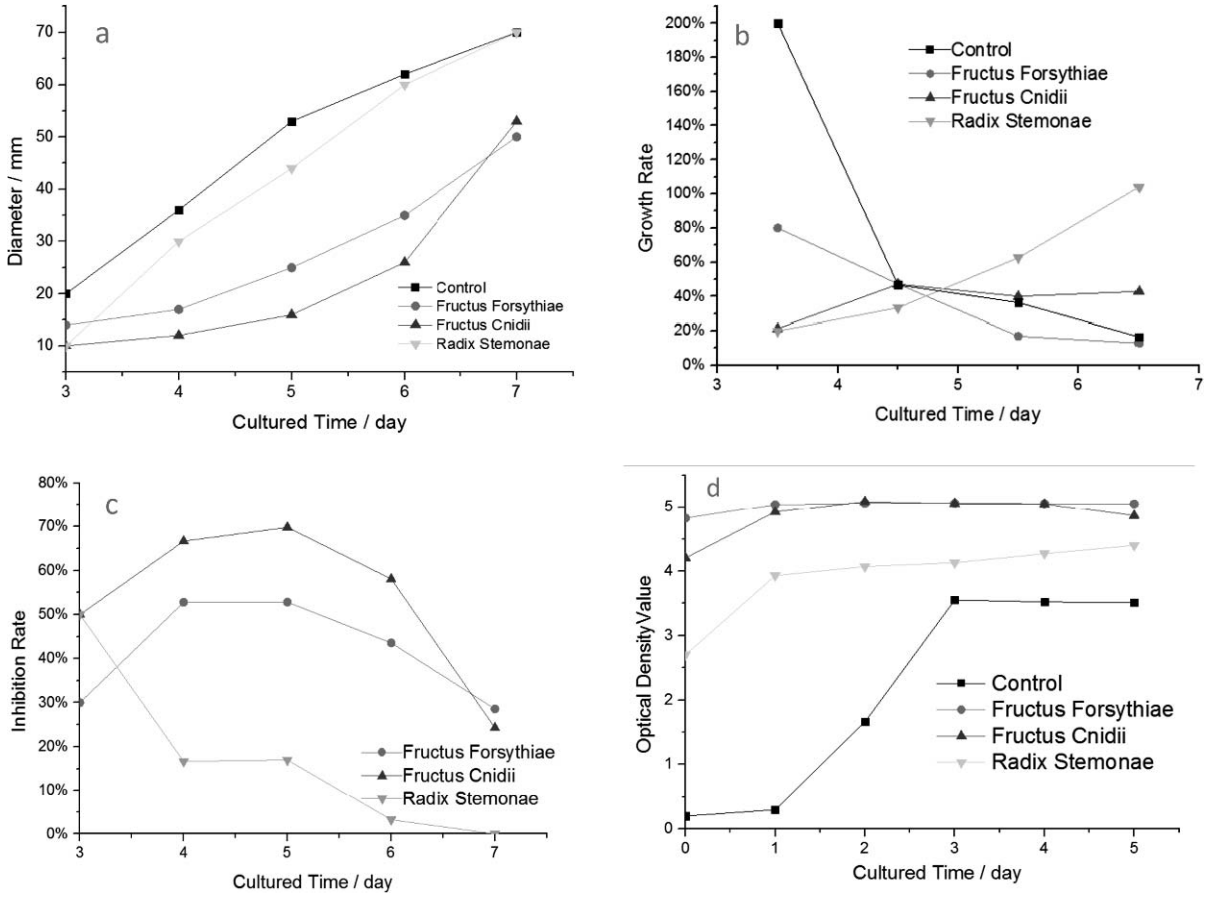

Figure 1.—Growth characteristics and inhibition efficiency of Trametes versicolor *in different media: (a) diameter, (b), growth rate, (c) inhibition rate, and (d) optical density.*

branches and winding, and was arranged regularly using biological scanning electron microscopy (Fig. 3a). As shown in Figures 3b through 3f, the three Chinese herbal medicines have an apparent inhibitory effect on the morphology, growth, and development of white-rot fungus hyphae. Figures 3b and 3c show that after FC treatment, the hyphae are bunch-like, cross-linked, and arranged in complex ways, and the mycelium is sparse, wrinkled, and uneven in thickness, with many branches. Figures 3d and 3e show that the hyphae (treated by FF) are uneven in thickness, with many shriveled branches, and the surface wrinkles are clearly visible. Figure 3f expresses that the hyphae, treated by RS, are arranged in order, with no winding, uneven thickness, obvious fracture, and protrusion at the head end.

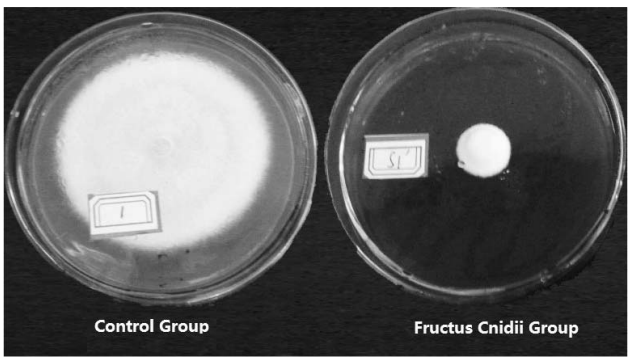

Figure 2.—Comparison of Trametes versicolor *growth deal by Fructus Cnidii media and control on day 6.*

Three types of traditional Chinese medicine clearly inhibit the morphology, growth, and development of white-rot fungi. FC had the most apparent antifungal effect on white-rot fungi, and all white-rot fungi were lethal on FC virulent medium. Other Chinese herbs also caused changes in the morphology of white-rot fungi hyphae and abnormal growth and development. Hyphae vary in thickness; number of branches; degree of shriveling, surface wrinkling, and intricateness of arrangement; bundle growth; and winding. Because the active ingredients in Chinese herbal medicine participate in the metabolism of substance and energy in mycelium, it affects normal mycelium growth and causes abnormal mycelium development. The main possible reason for achieving an excellent antifungal effect is the morphological toxicological effect of three Chinese herbal medicine preservatives on wood white-rot fungi.

Two-dimensional gel electrophoresis maps

Figures 4 and 5 show typical gel maps for TV proteins in the control and FC culture medium, with differentially expressed proteins circled in red on both maps. There were 293 proteins in healthy strains and 275 proteins in FC-

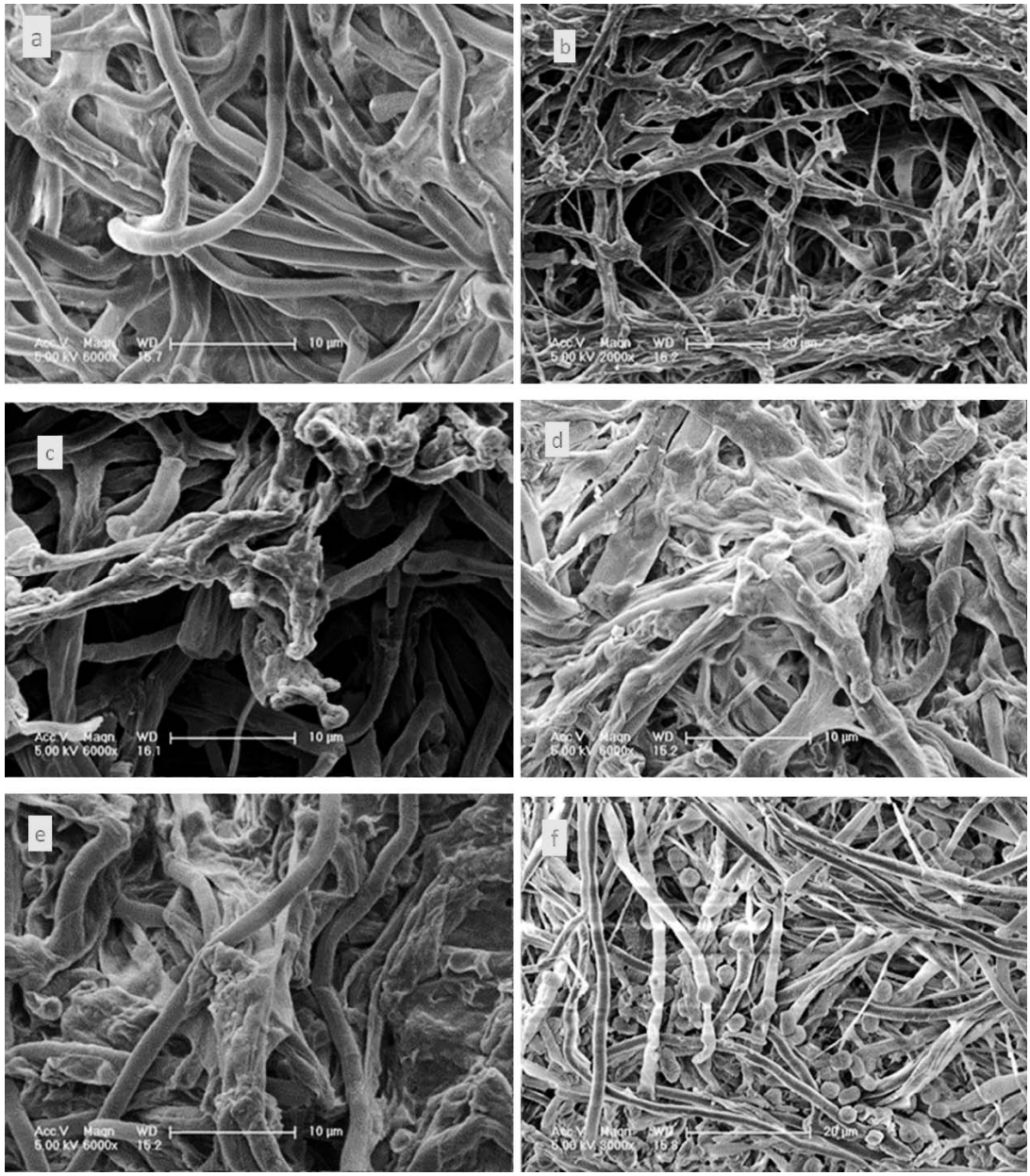

Figure 3.—Scanning electron microscopic observations for Trametes versicolor *with different media: (a) control, (b)* Fructus Cnidii*, (c)* Fructus Cnidii*, (d)* Fructus Forsythiae*, (e)* Fructus Forsythiae*, and (f) Radix Stemonae*.

treated strains, with 184 matching points, and the matching rate is 65.493 percent.

Comparing these two maps shows that there are many points where differences can be observed, indicating that the protein expression in white-rot fungus changes strongly after being treated with FC. Among them, 14 proteins were expressed as three times more different, of which eight of them were upregulated and six downregulated. These were distributed mainly in the PI 4–7, MW 15–80 KD region. Detailed information and the differential multiple of differential proteins are shown in Table 1. In addition, there were 10 isolate-specific proteins for control strains and 20 isolate-specific proteins for FC-treated TV.

In summary, the expression of proteins and enzymes involved in DNA synthesis is affected by the pharmacological effects of FC. Alternatively, some peptides are destroyed, causing the disappearance or relative increase of some proteins, affecting proteins required for cell division, and, finally, disintegrating the fungus to achieve the antifungal effect. Based on the previous study, the possible active components for antifungals are osthole and imperatorin, which are the main active ingredients of FC and have been found in antifungals, antivirals, and broad-spectrum antimicrobials (Zhou et al. 2005, Han et al. 2011, Zhang et al. 2017). These findings are consistent with previous research on antifungal properties of wood decay fungi in *Coptis*, *Sophora flavescens*, *Cnidium monnieri*, *Forsythia suspensa*, *Kochia scoparia*, and *Stemona* (Weickhardt et al. 1996, Schulze et al. 2021) and have implications for the development of natural wood preservatives.

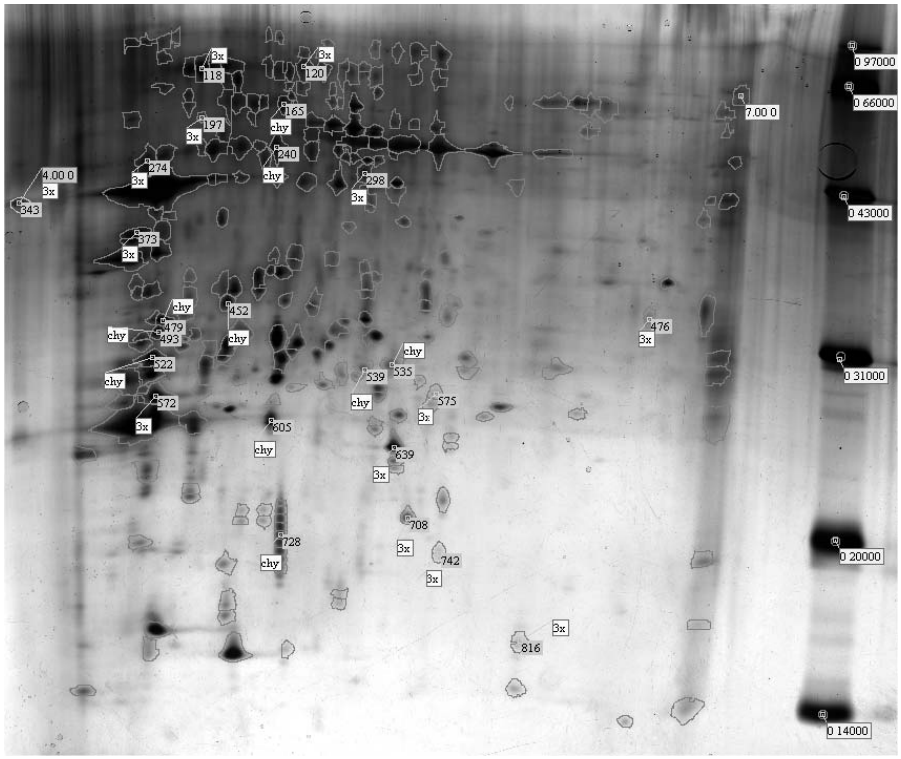

Figure 4.—Two-dimensional electrophoresis gel map of control group (C.mel).

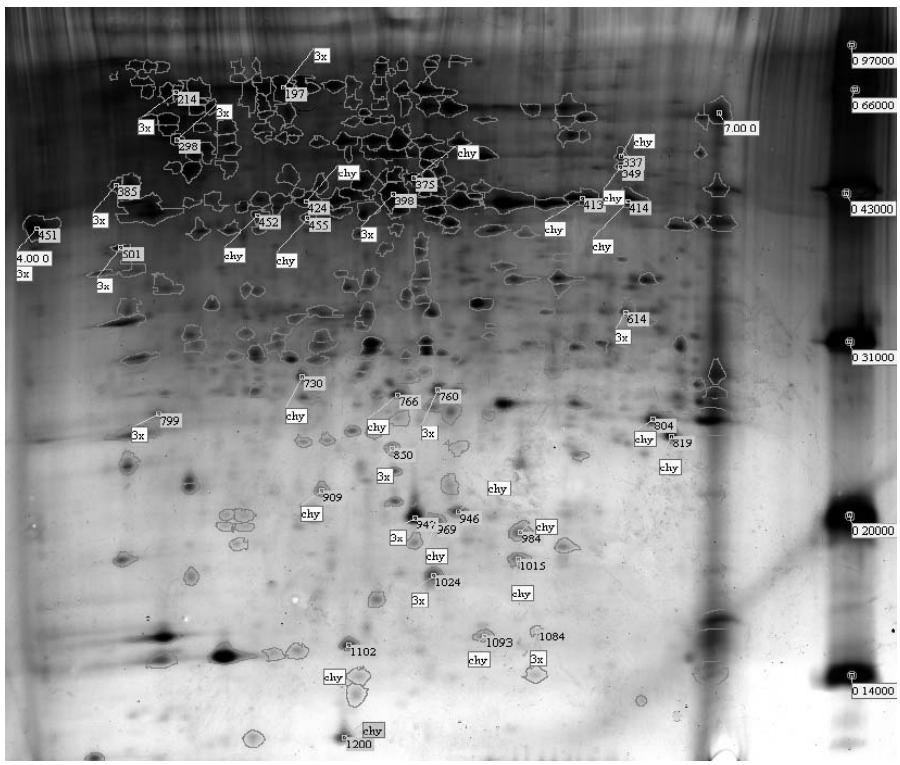

Figure 5.—Two-dimensional electrophoresis gel map of Fructus Cnidii *group (F.mel).*

Table 1.—Differentially expressed proteins with differential multiple (DM) more than three times.

Gel name	SpotID	X	Y	Area	Volume (%)	pI	MW	Intensity (%)	DM
C.mel	118	897	353	22.5241	0.86238	4.76199	78,062	0.539496	−9.01989
F.mel	214	700	495	7.06853	0.095609	4.60743	65,247	0.147065	
C.mel	120	1,284	345	17.008	0.212361	5.18387	79,618	0.262124	4.33429
F.mel	197	1,097	475	26.8467	0.920435	5.08307	67,320	0.397361	
C.mel	197	895	539	4.69354	0.025823	4.75981	58,464	0.110348	4.75346
F.mel	298	704	683	7.4274	0.122748	4.61222	53,635	0.220487	
C.mel	274	687	705	26.4999	0.585961	4.53307	49,297	0.305241	−6.52892
F.mel	385	481	865	11.1492	0.089749	4.34505	44,366	0.108945	
C.mel	298	1,517	751	14.5161	0.243321	5.43786	47,021	0.387124	5.01714
F.mel	398	1,500	899	34.2822	1.22077	5.56589	42,905	0.376808	
C.mel	343	198	865	14.0403	0.300907	4.00000	42,392	0.420806	4.56118
F.mel	451	193	1,034	37.6169	1.37249	4.00000	39,805	0.438467	
C.mel	373	646	977	15.2016	0.412548	4.48837	39,958	0.390424	−3.86795
F.mel	501	494	1,112	5.99192	0.106658	4.36062	38,117	0.385783	
C.mel	476	2,602	1,309	11.9476	0.118395	6.62064	33,536	0.205092	3.15281
F.mel	614	2,352	1,369	15.7742	0.373276	6.58666	33,045	0.490836	
C.mel	572	721	1,601	28.4475	1.47663	4.57013	28,308	0.874671	−7.17952
F.mel	799	635	1,771	12.7177	0.205673	4.52955	25,827	0.288518	
C.mel	575	1,793	1,592	10.7621	0.102349	5.73874	28,471	0.212708	5.16771
F.mel	760	1,662	1,674	13.7822	0.528911	5.75998	27,471	0.548084	
C.mel	639	1,626	1,795	16.5322	0.987624	5.55669	25,027	1.094220	−3.25899
F.mel	850	1,496	1,908	10.3387	0.303046	5.5611	23,672	0.459020	
C.mel	708	1,680	2,065	11.9113	0.46516	5.61555	21,083	0.716290	3.15371
F.mel	947	1,580	2,184	19.8185	1.46698	5.66174	19,877	0.988154	
C.mel	742	1,803	2,201	13.3387	0.170799	5.74964	19,436	0.232421	3.58132
F.mel	1,024	1,648	2,412	14.1613	0.611685	5.74321	17,484	0.633322	
C.mel	816	2,111	2,529	16.5403	0.218992	6.08539	16,283	0.268217	−3.22423
F.mel	1,084	2,027	2628	5.46773	0.067921	6.19728	15,483	0.169818	

Conclusions

In conclusion, the antifungal ability of three Chinese medicine herbals, Fructus Cnidii, Fructus Forsythiae, and Radix Stemonae, was reported. Batch experiments analyzed the growth characteristics, morphological properties, and protein expression characteristics. These experiments confirmed that Fructus Cnidii exhibits the best antifungal activity for *T. versicolor*. The mycelium appeared uneven in thickness, shriveled, wrinkled on the surface, and intricately arranged and grew in bundles after treatment. In addition, the results identified that the Chinese herbal medicine used in this study expressed inhibition ability rather than direct killing, and the electrophoresis maps show that Fructus Cnidii affected the expression of protein and enzymes to achieve antifungal ability. Overall, Chinese medicine herbs could provide a base for future research and development of green wood preservatives, but further work is needed on prolonging the inhibition time.

Acknowledgments

This study was financially supported by the Natural Science Foundation of Inner Mongolia (2018MS03048) and the Science and Technology Innovation Guidance Project of Inner Mongolia. The authors would also like to thank the National Key Research and Development Program of China (2016YFD0600904).

Literature Cited

Baldrian, P. 2003. Interactions of heavy metals with white-rot fungi. *Enzyme Microb. Technol*. 32(1):78–91.

Broda, M. 2020. Natural compounds for wood protection against fungi—A review. *Molecules* 25(15):3538.

Ekor, M. 2014. The growing use of herbal medicines: Issues relating to adverse reactions and challenges in monitoring safety. *Front. Pharmacol*. 4:177.

Goodell, B. 2003. Brown-rot fungal degradation of wood: Our evolving view. *ACS Symp. Ser*. 845. DOI:10.1021/bk-2003-0845.ch006

Goodell, B., Y. Qian, and J. Jellison. 2008. Fungal decay of wood: Soft rot—brown rot—white rot. *ACS Symp. Ser*. 982:9–31.

Green, F., III and C. A. Clausen. 2003. Copper tolerance of brown-rot fungi: Time course of oxalic acid production. *Int. Biodeterior. Biodegrad*. 51(2):145–149.

Green, F., III and T. L. Highley. 1997. Mechanism of brown-rot decay: Paradigm or paradox. *Int. Biodeterior. Biodegrad*. 39(2–3):113–124.

Han, L., Y. F. Feng, W. Rui, H. M. Liang, and Z. F. Shi. 2011. Analysis of the constituents of Fructus Cnidii extract by in vitro and in vivo UPLC/Q-TOF-MS/MS. *Lishizhen Med. Mater. Med. Res*. 22(2):287–289.

Jellison, J., J. Connolly, B. Goodell, B. Doyle, B. Illman, E. Fekete, and A. Ostrofsky. 1997. The role of cations in the biodegradation of wood by the brown rot fungi. *Int. Biodeterior. Biodegrad*. 39(2–3):165–179.

Jiang, S. Y., X. M. Wang, and Y. M. Wang. 2014. Antifungal activities of 20 kinds of Chinese herbal extracts of water wood white-rot fungi and wood brown-rot fungi. *Wood Process. Machinery* 25(5):33–35.

Khan, M. R., M. Kihara, and A. D. Omoloso. 2001a. Antimicrobial activity of *Psychotria microlabastra*. *Fitoterapia* 72(7):818–821.

Khan, M. R., M. Kihara, and A. D. Omoloso. 2001b. Antimicrobial activity of *Cassia alata*. *Fitoterapia* 72(5):561–564.

Khan, M. R., M. Kihara, and A. D. Omoloso. 2002. Antimicrobial activity of *Michelia champaca*. *Fitoterapia* 73(7–8):744–748.

Macchioni, N., B. Pizzo, and C. Capretti. 2016. An investigation into preservation of wood from Venice foundations. *Construction Building Mater*. 111:652–661.

Penttilä, P. A., M. Altgen, M. Awais, M. Österberg, L. Rautkari, and R. Schweins. 2020. Bundling of cellulose microfibrils in native and polyethylene glycol-containing wood cell walls revealed by small-angle neutron scattering. *Sci. Rep*. 10(1):1–9.

Schulze, W. X., M. Altenbuchinger, M. He, M. Kränzlein, and C. Zörb. 2021. Proteome profiling of repeated drought stress reveals genotype-

specific responses and memory effects in maize. *Plant Physiol. Biochem*. 159:67–79.
Shen, D., N. Li, Y. Fu, N. Macchioni, L. Sozzi, X. Tian, and J. Liu. 2018. Study on wood preservation state of Chinese ancient shipwreck Huaguangjiao I. *J. Cultural Heritage* 32:53–59.
Sinha, S., T. Murugesan, K. Maiti, J. R. Gayen, B. Pal, M. Pal, and B. P. Saha. 2001. Antibacterial activity of *Bergenia ciliata* rhizome. *Fitoterapia* 72(5):550–552.
Teng, T. J., M. N. M. Arip, K. Sudesh, A. Nemoikina, Z. Jalaludin, E. P. Ng, and H. L. Lee. 2018. Conventional technology and nanotechnology in wood preservation: A review. *BioResources* 13(4):9220–9252.
Wachenheim, D. E., J. A. Patterson, and M. R. Ladisch. 2003. Analysis of the logistic function model: derivation and applications specific to batch cultured microorganisms. *Bioresour. Technol*. 86(2):157–164.
Weickhardt, C., F. Moritz, and J. Grotemeyer. 1996. Time-of-flight mass spectrometry: State-of the-art in chemical analysis and molecular science. *Mass Spectrom. Rev*. 15(3):139–162.
Zhang, L., A. Sun, A. Li, J. Kang, Y. Wang, and R. Liu. 2017. Isolation and purification of osthole and imperatorin from Fructus Cnidii by semi-preparative supercritical fluid chromatography. *J. Liq. Chromatogr. Relat. Technol*. 40(8):407–414.
Zhou, Y. H., Y. L. Li, and L. S. Wang. 2005. Analysis of chemical components of the essential oil from Fructus Cnidii. *J. Guangxi Univ. (Nat. Sci. Ed.)* 30(3):263.
Zwietering, M. H., I. Jongenburger, F. M. Rombouts, and K. J. A. E. M. Van't Riet. 1990. Modeling of the bacterial growth curve. *Appl. Environ. Microbiol*. 56(6):1875–1881.